

# Dielectric Properties of New Fully Conjugated 2H- and Metal-Pyrazinoporphyrazine Network Polymers

H. H. Abdel-Razik,<sup>1\*</sup> S. El-Sayed,<sup>2,3</sup> A. Hassen<sup>2,3</sup>

<sup>1</sup>Chemistry Department, Faculty of Science & Education (Alkhurma branch), Taif University, Saudi Arabia

<sup>2</sup>Physics Department, Faculty of Science & Education (Alkhurma branch), Taif University, Saudi Arabia

<sup>3</sup>Physics Department, Faculty of Science, Fayoum University, El Fayoum 63514, Egypt

Received 21 July 2010; accepted 10 January 2011

DOI 10.1002/app.34169

Published online 12 April 2011 in Wiley Online Library (wileyonlinelibrary.com).

**ABSTRACT:** 2,7-Di-*tert*-butylpyrene was oxidized to 2,7-di-*tert*-butylpyrene-4,5,9,10-tetraone. The latter through condensation reaction with vicinal diamine such as diaminomaleodinitrile afforded heterocyclic monomer, 2,7-di-*tert*-butylpyrene[4,5][9,10]bis(2,3-pyrazine-5,6-dinitrile), which was cyclotetramerized to the corresponding 2H- and metal-pyrazinoporphyrazine-based network polymers (2H-PyzPz and M-PyzPz, M = Co, Ni, Zn, or Cu). Elemental analytical results, Infrared, and NMR spectral data of the new prepared molecules are consistent with their assigned formulations. Molecular masses and metal contents of the synthesized polymers proved to be of high molecular masses, which confirm the efficiency of tetramerization polymerization and complexation reactions. Dielectric permit-

tivity,  $\epsilon'$ , loss tangent,  $\tan \delta$ , and ac conductivity,  $\sigma_{ac}(\omega)$ , of 2H-PyzPz and M-PyzPz films were studied as a function of temperature and frequency. It was found that dielectric permittivity,  $\epsilon'$ , decreases with the increase of frequency and increases with the increase in temperature. Ac conductivity,  $\sigma_{ac}(\omega)$ , is found to vary as  $B\omega^s$  and the frequency exponent,  $s$ , is less than unity around room temperature indicating a dominant hopping process. On the other hand,  $\sigma_{ac}(T)$  of all samples is thermally activated with low activation energies. © 2011 Wiley Periodicals, Inc. *J Appl Polym Sci* 121: 3579–3589, 2011

**Key words:** pyrazinoporphyrazine; metal-pyrazinoporphyrazine; dielectric permittivity; ac conductivity; hopping conduction mechanism

## INTRODUCTION

Tetrapyrazinoporphyrazine is one of the phthalocyanine derivatives having two nitrogen atoms at equivalent 1,4-positions of the phthalocyanine benzene units. Because of the additional nitrogen atoms, tetrapyrazinoporphyrazines are less electron-rich than the corresponding phthalocyanine.<sup>1</sup> Macroheterocycle systems such as porphyrins, tetrabenzoporphyrazines, and their aza analogs are interesting objects of extensive studies and practical applications, science, industry, and medicine. Porphyrine complexes of zinc, aluminum, and other metals show anticancer properties and uses in photodynamic therapy.<sup>2</sup>

The synthetic route to new fully conjugated systems can be achieved through condensation of diones with diamines. Hexa-1,5-diyne-3,4-diones react smoothly with commercially available diaminomaleodinitrile to give the dicyanodiethynylpyrazines.<sup>3</sup> Similarly, condensation of hexa-1,5-diyne-3,4-diones

with 4,5-diaminophthalonitrile produces 2,3-dialkynylquinoxaline-6,7-dinitriles.<sup>4</sup> Base-induced cyclotetramerization of the aromatic dinitriles with magnesium butoxide in refluxing butanol generates the peripherally peralkynylated phthalocyanine or naphthalocyanine analogs, namely, the tetrapyrazinoporphyrazines and tetra-6,7-quinoxalinoporphyrazines, respectively.<sup>5</sup> The pyrazinoporphyrazine system (metal-free, 2H-PyzPz, zinc and copper derivatives) has been synthesized by tetramerization of 2,3-dicyanopyrazine monomer unit.<sup>6</sup>

A new pyrazinoporphyrazine macrocycle carrying externally appended pyridine rings, tetrakis-2,3-[5,6-di(2-pyridyl)pyrazino]porphyrazine (hydrated) was prepared in high yield by direct cyclotetramerization of the precursor, 2,3-dicyano-5,6-di(2-pyridyl)-1,4-pyrazine, in the presence of 1,8-diazabicyclo[5.4.0]undec-7-ene (DBU).<sup>7</sup> Derivatives of the new class of octaalkynyltetra[6,7]quinoxalinoporphyrazines, analogs of the naphthalocyanines, were prepared in two steps starting from functionalized hexa-1,5-diyne-3,4-diones. Divalent zinc and magnesium ions were introduced into the macrocyclic core.<sup>8</sup> Condensation of diaminophthalonitrile with 1,10-phenanthroline-5,6-dione in EtOH afforded the suitably functionalized phthalonitrile precursor, as a pale yellow solid, which was cyclotetramerized in a refluxing solution of lithium metal dissolved in pentanol, followed by demetallation with acetic acid, affording the crude,

\*Present address: Chemistry Department, Faculty of Science (Damietta) 34517, Mansoura University, Egypt.

Correspondence to: H. H. Abdel-Razik (hamada600@yahoo.co.uk).

metal-free phthalocyanines, 2H-Pc, as a dark green solid.<sup>9</sup> Synthesis of tetra(5-*n*-nonyl-8-*tert*-butyl-2,3-pyrazino[2,3-*b*]indolo)porphyrinato copper(II) was reported.<sup>10</sup> Microporous polymeric materials were prepared through double aromatic nucleophilic substitution reaction of appropriate hydroxylated aromatic monomers with 4,5-dichlorophthalonitrile yielding a bis(phthalonitrile) precursor that forms a phthalocyanine network, via a cyclotetramerization by a metal ion template.<sup>11,12</sup> A highly conducting macrocycle-linked metallophthalocyanine polymer was reported.<sup>13</sup> It is known for most dielectrics that  $\epsilon'$ ,  $\tan \delta$ , and  $\sigma_{ac}$  are frequency and temperature dependent. Therefore, the dielectric characterizations of polymeric materials are crucial to study relevant mechanism of conduction and to realize their future applications. Measurements of  $\sigma_{ac}$  have been extensively used to understand the conduction mechanism of dielectric materials. The  $\sigma_{ac}(\omega)$  of most semiconductors shows a frequency  $\propto \omega^s$  with  $s \leq 1$ , where  $\omega$  is the angular frequency.<sup>14</sup> Different models such as small polaron tunneling (SPT), large polaron tunneling (LPT), correlated barrier hopping (CBH), atomic hopping, and quantum-mechanical tunneling (QMT) have been proposed to explain the behavior of ac conduction mechanism in different materials.<sup>15</sup> Ac electrical properties of metallophthalocyanines (M-Pc) such as Ni-Pc,<sup>16,17</sup> Co-Pc,<sup>18–20</sup> Zn-Pc,<sup>21,22</sup> and Cu-Pc<sup>23,24</sup> were reported earlier because these compounds have attracted much more interest in the last decades. Concerning the electrical behaviors, the outcome of these investigations can be summarized as follows: first, the ac conductivity shows  $\omega s$  dependence with  $s \leq 1$  indicating a hopping conduction mechanism at low temperatures and higher frequencies. Second, the conductivity is thermally activated with average activation energy,  $E < 1.0$  eV. Finally, the differences in the electrical behaviors of M-Pc ( $M = \text{Ni, Co, Zn, and Cu}$ ) are small. The present study seeks to underline the synthesis, characterization, and dielectric properties of the novel fully conjugated, pyrazinoporphyrazine-based network polymers.

## EXPERIMENTAL

### Characterization and sample preparation

Fourier-transform infrared spectrometer (8101 M-Shimadzu) was used in spectral measurements. UV–vis spectra were obtained using Unicam UV–vis spectrometer. NMR spectra were recorded in deuteriochloroform, on a Varian VXR 400S-NMR spectrometer operating at 400 MHz (<sup>1</sup>H-NMR) and 100 MHz (<sup>13</sup>C-NMR) with tetramethylsilane as internal standards. Elemental analysis for metal content was carried out by an inductively coupled plasma–atomic

emission spectroscopy (ICP-AES), using a Varian Liberty-100 sequential spectrometer. Molecular masses (number average  $M_n$ , weight average  $M_w$ ) were determined by gel permeation chromatography, GPC, (Polymer Laboratories, PL-GPC 20) using dilute polymer solutions (10 mg/5 mL) in tetrahydrofuran (THF) at room temperature with the rate of 1 mL min<sup>-1</sup>. Elemental analysis was determined with Perkin-Elmer 2400 CHN. Undoped and doped films were prepared by pouring the solution on a cleaned optically transparent glass plate. This glass plate was kept over a pool of mercury for perfect leveling to ensure uniform thickness, and the solution was allowed to evaporate at room temperature. Aluminum electrodes were deposited by vacuum evaporation at 10<sup>-6</sup> Torr, along the length of the glass plates, at the width of 3 mm, onto both surfaces of the samples to form a sandwich-type specimen in a cross-sectional area of  $2.5 \times 10^{-5}$  m<sup>2</sup> and thickness of 76  $\mu\text{m}$  for dielectric measurements.

Capacitance and dielectric loss tangent were measured in the frequency range from 100 to 1.0 MHz and within the temperature range from 303 to 423 K by using impedance spectroscopy of type Solartron 1260 gain/phase analyzer (Solartron Instruments, Allentown, PA). The dielectric constant was calculated from the given values of capacitance, thickness, and area of the sample. Knowing  $\epsilon'$ ,  $\tan \delta$ , and the frequency  $f$ , the ac conductivity was calculated,  $\sigma_{ac} = 2\pi f \epsilon_0 \epsilon' \tan \delta$ ,  $\epsilon_0$  is the permittivity of free space.

### Preparation of 2,7-di-*tert*-butylpyrene-4,5,9,10-tetraon 2

Pyrene was purchased from Acros and used as received. Other materials were obtained from Aldrich and used as received. 2,7-Di-*tert*-butylpyrene **1** was synthesized by using the reported procedure.<sup>25</sup> in greater than 90% yield. Compound **2** was prepared as previously reported.<sup>26</sup> To a solution of 2,7-di-*tert*-butylpyrene **1** (10 mmol) in CH<sub>2</sub>Cl<sub>2</sub> (40 mL) and CH<sub>3</sub>CN (40 mL) were added NaIO<sub>4</sub> (17.5 g, 81.8 mmol), H<sub>2</sub>O (50 mL), and RuCl<sub>3</sub>·*x*H<sub>2</sub>O (0.25 g, 1.2 mmol). The dark brown suspension was heated at 30–40°C overnight. The reaction mixture was poured into 500 mL of water, and the organic phase was separated. The aqueous phase was extracted with CH<sub>2</sub>Cl<sub>2</sub>. The CH<sub>2</sub>Cl<sub>2</sub> extracts were combined with the organic phase and washed with water to give a dark orange solution. The solvent was removed under reduced pressure to afford a dark orange solid. Column chromatography (CH<sub>2</sub>Cl<sub>2</sub>) gave pure product of compound **2** as bright orange crystals, mp 340–342°C.<sup>26</sup>

**Preparation of 2,7-di-*tert*-butylpyrene[4,5][9,10]-bis(2,3-pyrazine-5,6-dinitrile) 3**

A solution of tetraone **2** (10 mg, 0.027 mmol) in acetic acid (50 mL) was treated with diaminomaleodinitrile (5.83 mg, 0.054 mmol). The mixture was refluxed with stirring at room temperature for 2 h. The precipitate was filtered off and washed with acetic acid to give pale yellow solid. 13.83 mg, 89%; mp = 281°C.

IR (KBr):  $\nu$  cm<sup>-1</sup>, 2226 (CN), 1505 (C=N), 1614 (C=C). <sup>1</sup>H-NMR (CDCl<sub>3</sub>):  $\delta$  = 8.16 (s, aromatic-H), 1.53 (s, aliphatic-H); <sup>13</sup>C-NMR (CDCl<sub>3</sub>): 149.1 (C), 148.7 (C), 144.1 (C), 143.7 (C), 141.3 (C), 140.8 (C), 137.5 (C), 137.1 (C), 131.5 (C), 131.3 (C), 80.8 (C), 116.2 (CN), 35.7 (CH<sub>3</sub>), 32.8 (CH<sub>3</sub>). Anal. calcd. for C<sub>32</sub>H<sub>22</sub>N<sub>8</sub>: C, 74.12; H, 4.28; N, 21.61. Found: C, 74.14; H, 4.31; N, 21.59.

**Preparation of polytetra[2,3-(1,4-diazaphenanthreno)porphyrazine] 4**

Lithium metal (20 mg, 2.8 mmol) was added to a refluxing solution of **3** (259.28 mg, 0.5 mmol) in pentanol (2 mL). The solution was heated at reflux for 18 h. On cooling, acetic acid (0.2 mL) was added to the reaction mixture, and the crude product was collected by centrifugation. The green material was purified by column chromatography (eluent: dichloromethane) and by precipitation from toluene.

IR (KBr):  $\nu$  cm<sup>-1</sup>, 1515 (C=N), 3350 (NH), 1603 (C=C). UV-vis  $\lambda_{\max}$ (CH<sub>2</sub>Cl<sub>2</sub>) nm<sup>-1</sup>: 357, 438, 650, 698. <sup>1</sup>H-NMR (CDCl<sub>3</sub>):  $\delta$  = 9.77 (s, H, NH), 7.64 (s, aromatic-H), 1.39 (s, aliphatic-H). Anal. Calcd. for the expected polymer repeat C<sub>65</sub>H<sub>55</sub>N<sub>16</sub> requires C, 73.63; H, 5.23; N, 21.14. Found: C, 73.49; H, 5.17; N, 21.09.

**Preparation of polytetra[2,3-(1,4-diazaphenanthreno)porphyrazinato]-metal II 5a-d**

The monomer **3** (259.28 mg, 0.5 mmol) was subjected to form polymer networks **5a-d** on heating with 0.75 mmol of metal salt (cobalt II chloride, nickel II chloride, zinc acetate, or copper nitrate) in quinoline (2 mL) at 200°C for 18 h. The material was dissolved in acetone, and the untrapped metal was precipitated and removed from the solution. To the resulting acetone solution, an excess of cold methanol was added, precipitating blue (**5a**, **b**) or dark green (**5c**, **d**) solids. The solubility of these networks was examined in various solvents, showing that they are soluble in common organic solvents such as CH<sub>2</sub>Cl<sub>2</sub>, CHCl<sub>3</sub>, THF, and acetone at room temperature and are easily purified by chromatography on silica gel. The polymer was vacuum dried overnight.

5a

IR (KBr):  $\nu$  cm<sup>-1</sup>, 1504 (C=N), 1607 (C=C). UV-vis  $\lambda_{\max}$ (CH<sub>2</sub>Cl<sub>2</sub>) nm<sup>-1</sup>: 361, 446 (shoulder), 667, 725.

<sup>1</sup>H-NMR (CDCl<sub>3</sub>)  $\delta$  = 8.45 (s, aromatic-H), 1.46 (s, aliphatic-H). Anal. calcd. for the expected polymer repeat C<sub>65</sub>H<sub>53</sub>N<sub>16</sub>Co requires C, 69.88; H, 4.78; N, 20.06; Co, 5.28. Found: C, 64.74; H, 4.63; N, 19.94; Co, 5.43.

5b

IR (KBr):  $\nu$  cm<sup>-1</sup>, 1507 (C=N), 1605 (C=C). UV-vis  $\lambda_{\max}$ (CH<sub>2</sub>Cl<sub>2</sub>) nm<sup>-1</sup>: 360, 444 (shoulder), 663, 718. <sup>1</sup>H-NMR (CDCl<sub>3</sub>)  $\delta$  = 8.48 (s, aromatic-H), 1.44 (s, aliphatic-H). Anal. calcd. for the expected polymer repeat C<sub>65</sub>H<sub>53</sub>N<sub>16</sub>Ni requires C, 69.90; H, 4.78; N, 20.06, Ni, 5.25. Found: C, 69.68; H, 4.65; N, 19.97; Ni, 5.39.

5c

IR (KBr):  $\nu$  cm<sup>-1</sup>, 1505 (C=N), 1598 (C=C). UV-vis  $\lambda_{\max}$ (CH<sub>2</sub>Cl<sub>2</sub>) nm<sup>-1</sup>: 363, 447 (shoulder), 656, 709. <sup>1</sup>H-NMR (CDCl<sub>3</sub>)  $\delta$  = 8.44 (s, aromatic-H), 1.41 (s, aliphatic-H). Anal. calcd. for the expected polymer repeat C<sub>65</sub>H<sub>53</sub>N<sub>16</sub>Zn requires C, 69.48; H, 4.75; N, 19.95; Zn, 5.82. Found: C, 69.29; H, 4.72; N, 19.83; Zn, 5.96.

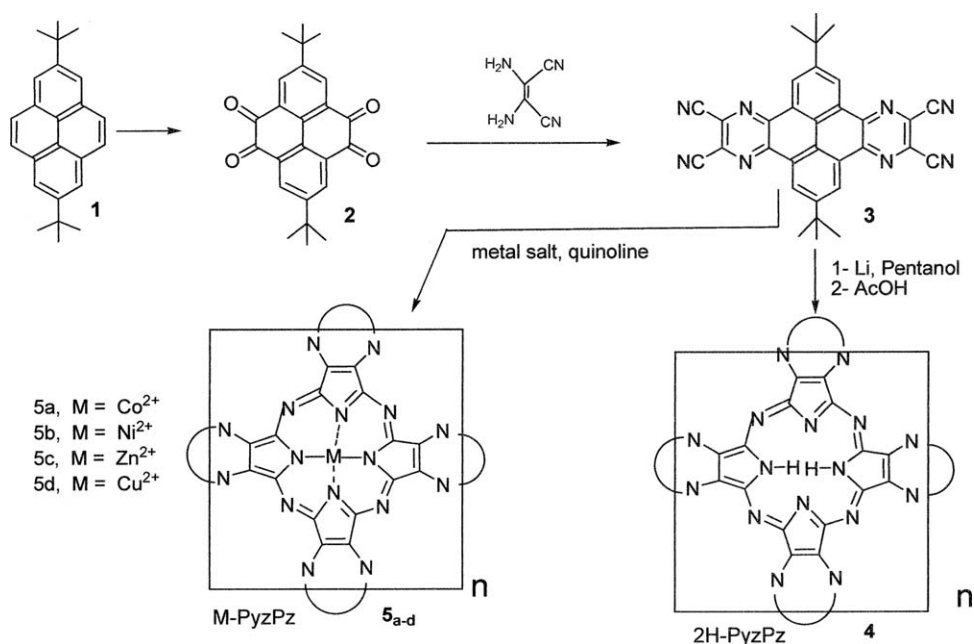
5d

IR (KBr):  $\nu$  cm<sup>-1</sup>, 1502 (C=N), 1604 (C=C). UV-vis  $\lambda_{\max}$ (CH<sub>2</sub>Cl<sub>2</sub>) nm<sup>-1</sup>: 366, 448 (shoulder), 654, 707. <sup>1</sup>H-NMR (CDCl<sub>3</sub>)  $\delta$  = 8.46 (s, aromatic-H), 1.45 (s, aliphatic-H). Anal. calcd. for the expected polymer repeat C<sub>65</sub>H<sub>53</sub>N<sub>16</sub>Cu requires C, 69.60; H, 4.76; N, 19.98; Cu, 5.66. Found: C, 69.45; H, 4.75; N, 19.87; Cu, 5.78.

**RESULTS AND DISCUSSIONS**

We report here, the synthesis, characterization, and dielectric properties of the novel fully conjugated, network polymers of tetramerized metal-free pyrazinoporphyrazine, 2H-PyzPz, and metal-pyrazinoporphyrazine, M-PyzPz, containing four peripheral diimine binding sites. The synthetic route to these network polymers is summarized in Scheme 1. The key intermediate in the synthesis is the precursor 2,7-di-*tert*-butylpyrene[4,5][9,10]bis(2,3-pyrazine-5,6-dinitrile) **3**. The starting material is 2,7-di-*tert*-butylpyrene **1**, which was synthesized by using the reported procedure.<sup>25</sup> Compound **1** was converted in the first step to 2,7-di-*tert*-butylpyrene-4,5,9,10-tetraone **2**<sup>26</sup> by treatment with NaIO<sub>4</sub> and RuCl<sub>3</sub>·xH<sub>2</sub>O.

Condensation of **2** with commercially available diaminomaleodinitrile in acetic acid afforded the suitably functionalized pyrene[4,5][9,10]bis(2,3-pyrazine-5,6-dinitrile) **3**, as a pale yellow solid. Cyclotramerization of the aromatic tetranitrile **3** with lithium metal in pentanol and metal salt in quinoline



**Scheme 1** 2H- and metal-pyrazinoporphyrazine network polymers from heterocyclic monomer.

generates 2H-PyzPz **4** and M-PyzPz **5a-d** network polymers, respectively.

### Infrared and UV-vis spectrum

The IR spectral data of precursor **3** shows an intense bands at 2226, 1505, and 1614  $\text{cm}^{-1}$  for  $\text{C}\equiv\text{N}$ ,  $(\text{C}=\text{N})$ , and  $(\text{C}=\text{C})$  groups, respectively. In accordance with this structure, the  $^1\text{H-NMR}$  spectrum revealed a singlet at  $\delta = 8.16$  and 1.53 assignable to aromatic and aliphatic protons, respectively. Elemental analytical results and  $^{13}\text{C-NMR}$  spectral data of the new tetranitrile **3** are consistent with the assigned formulation (see Experimental, Scheme 1). IR spectrum of 2H-PyzPz **4** shows a broad band at 1515  $\text{cm}^{-1}$ , which is assignable to the stretching vibration of the  $\text{C}=\text{N}$  bond. The absorption values of the  $\text{C}=\text{N}$  vibration at 1504, 1507, 1505, and 1502  $\text{cm}^{-1}$  for Co-PyzPz **5a**, Ni-PyzPz **5b**, and Zn-PyzPz **5c** and Cu-PyzPz **5d** respectively, are lower by about 8–13  $\text{cm}^{-1}$  than those for the metal-free 2H-PyzPz **4**, which indicate the coordination of azomethine nitrogen atom to metal ions in the complexes. Moreover, there is a broad band at 3350  $\text{cm}^{-1}$ , assignable to the stretching vibration of the  $\text{N-H}$  bond in free metal pyrazinoporphyrazine complex 2H-PyzPz **4**. This stretching vibration of the  $\text{N-H}$  bond does not appear in the spectra of metal complexes **5a-d**, which means that  $\text{NH}$  group is involved in metal-ligand formation. UV-vis spectrum of 2H-PyzPz **4** in dichloromethane solution shows a strong Soret bands at 357 and 438 nm (Fig.1). The Q bands attributable to the difference between the highest occupied molecular orbital (HOMO) energy level and the

lowest unoccupied molecular orbital (LUMO) energy, that is, the  $\pi-\pi^*$  transitions in 2H-PyzPz **4** are observed at 650 and 698 nm. These bands are in a good agreement with the absorption spectra reported in the literature.<sup>10</sup>

The electronic absorption spectra of the metal complexes **5a-d** in dichloromethane solution are presented in Figure 2. Two transitions are dominated at higher-energy B-band (broad band around 363 nm and shoulder band around 446 nm) which can be assigned to the  $\pi-\pi^*$  and/or  $d-\pi^*$  transitions in the fused pyrolopyrazine ring structure.<sup>27,28</sup> Two characteristic well-developed intense

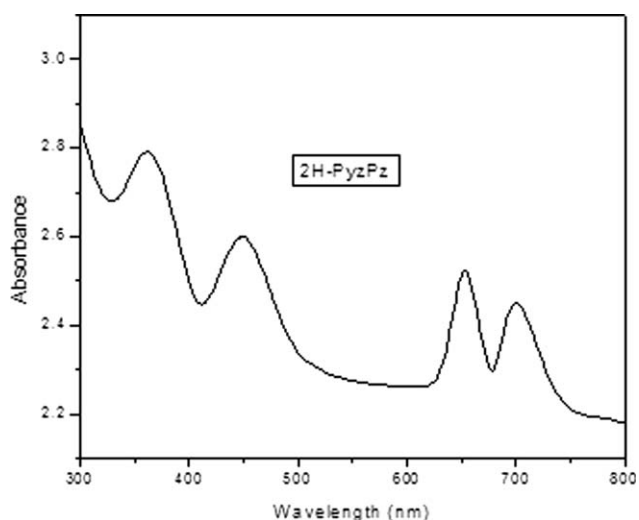


**Figure 1** UV-vis spectra of metal free-pyrazinoporphyrazine **4**.

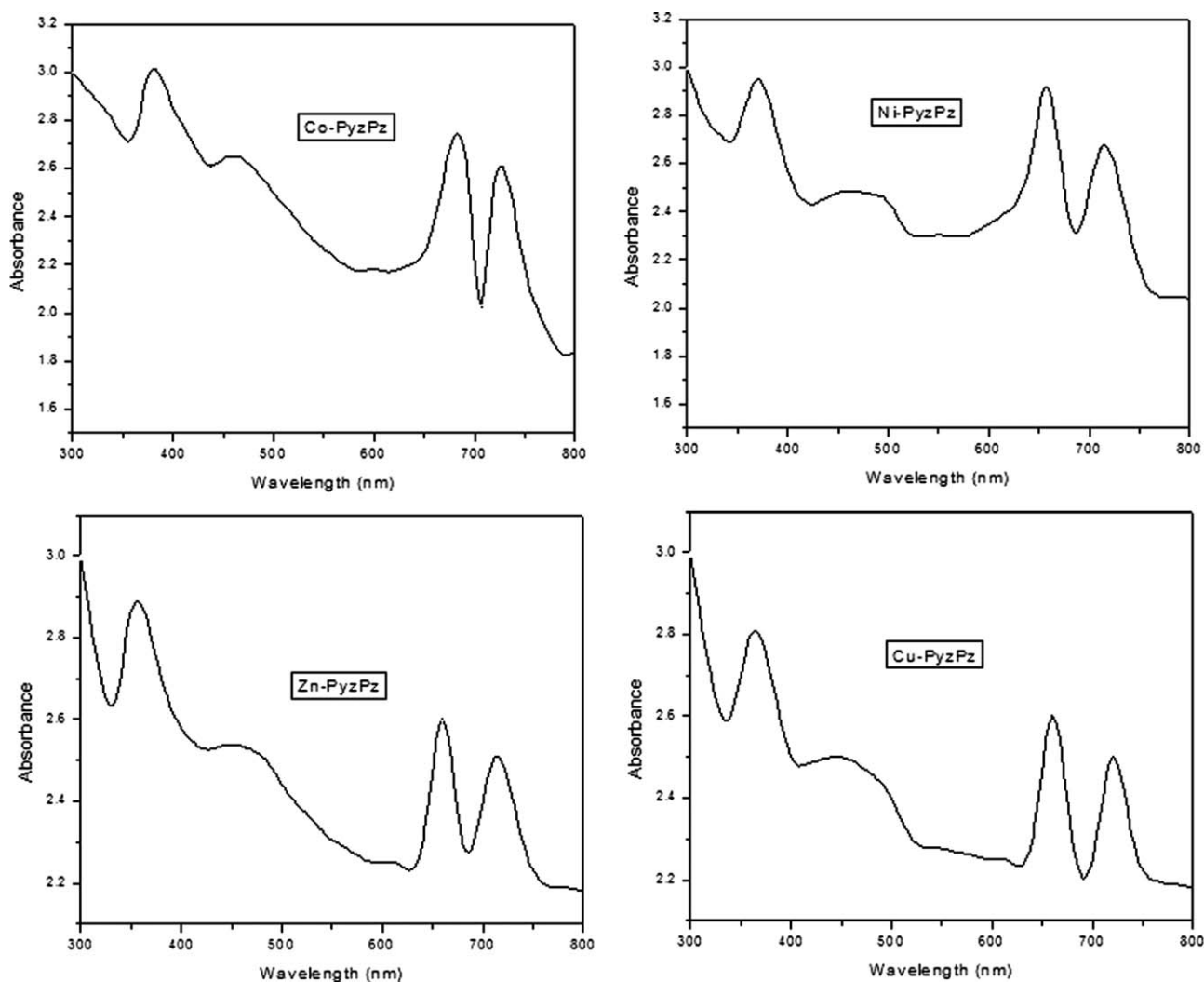


Figure 2 UV-vis spectra of metal-pyrazinoporphyrazines (M-PyzPz) 5a-d.

lower-energy Q-bands ( $\sim 663$  and  $718$  nm) are observed. The shoulder band is usually attributed to the  $1s \rightarrow 4d$  transition.<sup>29</sup> It was already demonstrated in early theoretical work,<sup>30,31</sup> that exchange coupling of the metal center with ligand states gives rise to spin-allowed transitions at low energy. It will be shown that there are states in the range of 450–480 nm below the Q-band excitation for all of the M-PyzPz polymers. These states arise from  $d-d$  excitations and ligand-metal exchange coupling.

There is a little difference among the visible spectra of various metal pyrazinoporphyrazines (Figure 2). It has been suggested that both Q and B bands can be influenced by the metal-to-ligand charge-transfer bands.<sup>32</sup> It is clear that the absorption bands for metal complexes, extends beyond 800 nm. Therefore, these pyrazinoporphyrazines could be useful in the field of optical data storage and for security printing, which require absorbance in the near infrared.

#### <sup>1</sup>H-NMR and molecular mass measurements of the prepared network polymers

<sup>1</sup>H-NMR spectrum of 2H-PyzPz **4** reveals signals at  $\delta = 7.64$  and  $1.39$  assignable to aromatic and aliphatic protons, respectively. The presence of signal at  $\delta = 9.77$  assignable to NH proton in <sup>1</sup>H-NMR spectrum of 2H-PyzPz **4** gives direct evidence of the formation of an unsymmetrical tetradentate ligand. On the formation of metal complexes **5a-d**, the signal of the NH groups disappears. All metal complexes show signals around  $\delta = 8.46$  and  $1.44$  assignable to aromatic and aliphatic protons, respectively (see Experimental, Scheme 1 and Fig. 3). Elemental analyses for the prepared polymers show that the amount of carbon within polymers is consistent with their idealized structures represented in Scheme 1. The experimental values of carbon content of the prepared polymers are consistent with that calculated for the expected polymer repeat unit. Also, the experimental values of metal content (see Experimental) of the prepared polymers are consistent

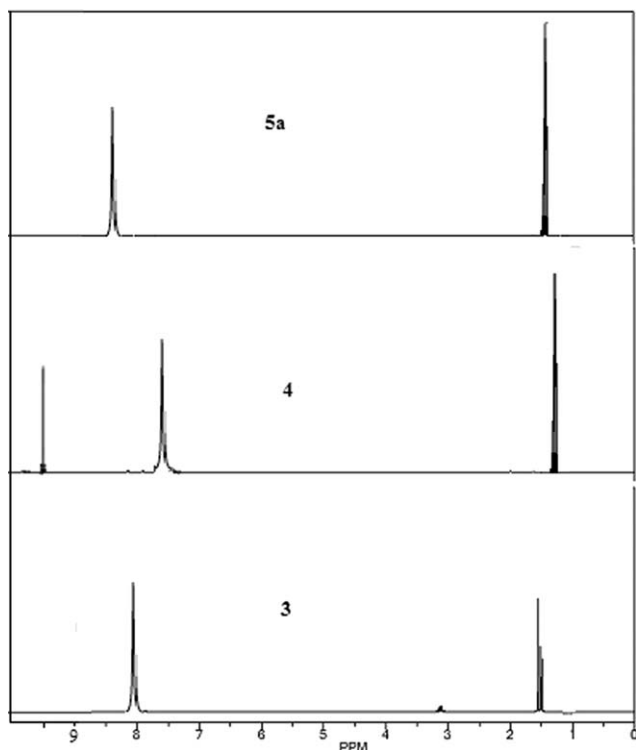


**Figure 3**  $^1\text{H}$ NMR spectra of the prepared pyrene derivative 3, 2H-PyzPz 4 and Co-PyzPz 5a.

with that calculated for the expected polymer repeat unit. Moreover, metal content and high molecular masses of the synthesized polymers confirm the efficiency of tetramerization polymerization and complexation reactions. The narrow molecular weight distribution (Table I) in all samples, with  $M_w/M_n = 3.58\text{--}4.45$ , implies that the polymerization follows a single-site reaction mechanism. The high molar mass and good solubility of these polymers allow conventional solution-based polymer processing techniques.

These pyrazinoporphyrazines have push-pull intramolecular charge-transfer chromophoric systems in which the pyrene and the pyrazine rings work as a donor group and an acceptor group, respectively. Hence, these polymeric materials exhibit high electrical conductivity. The special conjugation in pyrazinoporphyrazines enables the electrons to delocalize throughout the whole system. In addition, the delocalized electrons may move around the whole network polymers to make them conductive. When the electrons are removed from the backbone, resulting in cations or added to the backbone resulting in anions, the polymer can be transformed into a conducting form. Anions and cations act as charge carriers, hopping from one site to another under the influence of an applied electrical field, thus increasing conductivity. It is universally agreed that the doping process is an effective

method to produce conducting polymers, because it allows electrons to flow through the conduction bands. As doping occurs, the electrons in the conjugated systems, which are loosely bound, are able to jump around the polymer chains.

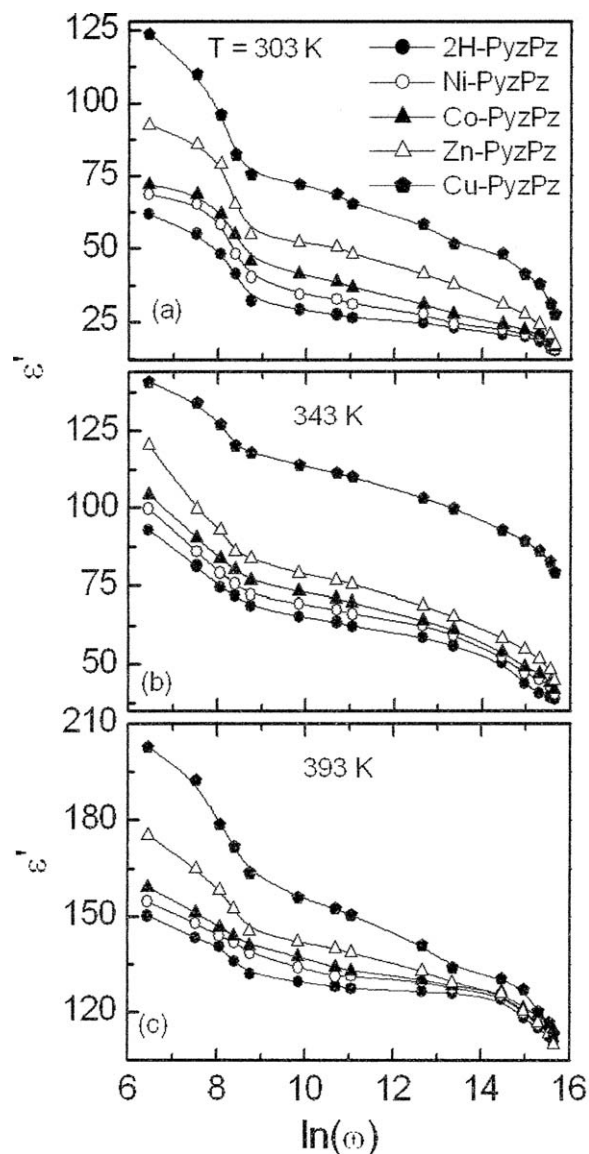
### Dielectric permittivity

Figure 4(a–c) displays the temperature dependence of the real part of the permittivity ( $\epsilon'$ ) at some selected frequencies. It is clear that  $\epsilon'(\omega)$  decreases with the increase of frequencies for all investigated network samples. The decrease of  $\epsilon'(\omega)$  with frequency at given temperatures may be attributed to the decrease in the number of the dipoles, which contribute to polarization. Also, the dipole structure is no longer able to respond to the applied electric field. Because the material electrode polarization cannot be ignored in ionic conductors, the decrease of  $\epsilon'(\omega)$  with the increase in frequency may be attributed to relaxation processes.<sup>33</sup> Moreover, the variation of  $\epsilon'(\omega)$  is small at higher frequencies. Therefore, the difference between  $\epsilon'(\omega)$  of 2H-PyzPz and that of M-PyzPz samples is not pronounced. It is also worth noting that the  $\epsilon'(\omega)$  tends to become largely noticeably with the increase of temperature. The presence of metal ions such as Ni, Co, Zn, and Cu leads to increase the values of  $\epsilon'(\omega)$  at the lower frequencies. Cu-PyzPz shows higher values of  $\epsilon'(\omega)$  in comparison with 2H-PyzPz or other M-PyzPz samples. A dispersion in  $\epsilon'(\omega)$  around 1.0 kHz, is recognized for investigated samples due to electrical relaxation. Higher values of  $\epsilon'(\omega)$  reflect the conductive nature of pyrazinoporphyrazines.

Figure 5(a–c) depicts the temperature dependence of  $\epsilon'(T)$  at some selected frequencies (1, 10, and 100 kHz) for 2H-PyzPz and M-PyzPz samples. It is shown that  $\epsilon'(T)$  increases with the increase in temperature and the decrease in frequency. A similar behavior is observed for bulk tin phthalocyanine dichloride ( $\text{SnPcCl}_2$ ).<sup>34</sup> Again, Cu-PyzPz exhibits higher  $\epsilon'$  compared to 2H-PyzPz or other M-PyzPz networks. The rate of increase in  $\epsilon'(T)$  with temperature ( $d\epsilon'/dT$ ) undergoes a pronounced change at  $T =$

**TABLE I**  
Characteristic Data of the Prepared  
Pyrazinoporphyrazine Network Polymers

Samples	Yield (%)	Mp (°C)	$M_n$ (g mol <sup>-1</sup> )	$M_w$ (g mol <sup>-1</sup> )	Polydispersity ( $M_w/M_n$ )
2H-PyzPz	89	212–214	26,945	111,544	4.139
Co-PyzPz	83	237–236	27,462	118,233	4.305
Ni-PyzPz	84	254–255	36,766	131,654	3.580
Zn-PyzPz	93	246–248	38,457	147,623	3.838
Cu-PyzPz	90	274–276	31,372	139,694	4.452



**Figure 4** The frequency dependent of  $\epsilon'$  for 2H-PyzPz and M-PyzPz networks at different Temperatures; (a)  $T = 303$  K, (b)  $T = 343$  K, and (c)  $T = 393$  K.

325.5 K,  $f = 1.0$  and 10.0 kHz. Moreover, a slight change in  $d\epsilon'/dT$  at  $T = 378$  K for all networks is observed. This change can be attributed to the local main-chain dynamic. Since a rapid increase in  $\epsilon'(T)$  begins near to the glass-transition temperature of polymeric materials. It might be suggested that  $T_g$  of both 2H-PyzPz and M-PyzPz is around 325.5 K. Only one peak of  $d\epsilon'/dT$  is found at 363 K and 100 kHz for all samples as shown from the inset of Figure 5(c). This peak may be attributed to  $\alpha$ -relaxation. A similar increase in  $\epsilon'(T)$  for phthalocyanine compounds was reported<sup>34</sup> and attributed to the phase transformation from  $\alpha$ - to  $\beta$ -phase. The temperature coefficient of permittivity (TCP) for all network samples at different frequencies is obtained by using the relation:

$$TCP = \frac{1}{\epsilon'} \frac{d\epsilon'}{dT} \quad (1)$$

where  $\epsilon'$  is the value of the dielectric constant at the half of the maximum peak and  $d\epsilon'/dT$  is the change of  $\epsilon'$  with temperature. It was found that TCP of all samples is about  $0.06 \text{ K}^{-1}$  and slightly dependent on frequency.

#### Dielectric loss tangent

The dielectric losses in most polymeric materials can be attributed to the perturbation of phonons by the application of the electric field and so, the energy transferred to phonon dissipation in the form of

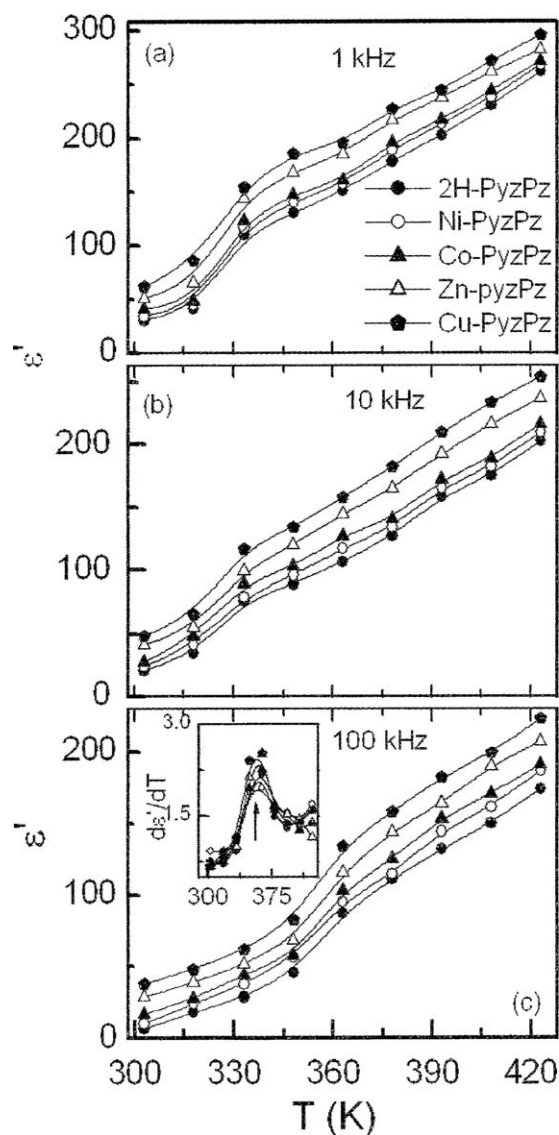


**Figure 5** The temperature dependence of  $\epsilon'$  for 2H-PyzPz and M-PyzPz samples at different frequencies: (a) 1.0 kHz, (b) 10 kHz, and (c) 100 kHz. The inset in (c) depicts the change of  $d\epsilon'/dT$  versus temperature at 100 kHz for all investigated samples.

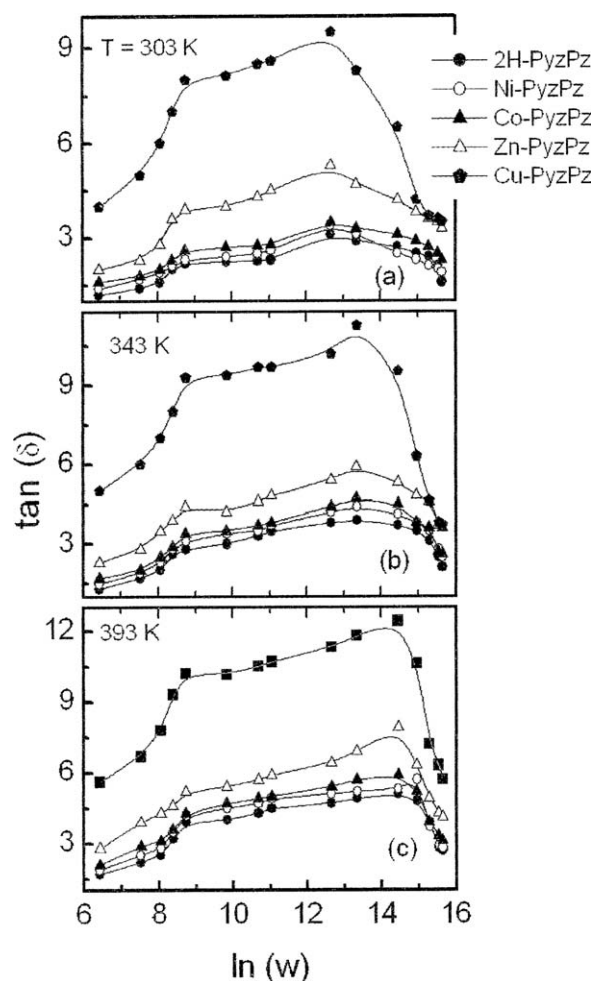


**Figure 6** The frequency dependent of  $\tan \delta$  for 2H-PyzPz and M-PyzPz samples at different temperatures; (a)  $T = 303$  K, (b)  $T = 343$  K, and (c)  $T = 393$  K.

heat. Besides, macromolecules modify the perturbation of phonon during application of electric field.<sup>35</sup> Figure 6(a–c) represents the frequency dependence of  $\tan \delta$  at some selected temperatures (303, 343, and 393 K) for all samples. The variation of  $\tan \delta$  with frequency gives evidence for dipolar peak with position slightly temperature dependent. For all investigated samples, this peak is located at higher frequencies ( $f = 50, 100,$  and  $300$  kHz) when  $T$  is 303, 343, and 393 K, respectively. Because of molecular weights distribution or cooperative movement of adjacent chains a spread of relaxation times occurs. Also, a shoulder peak is shown at 1.0 kHz for all samples at selected temperatures. The existence of this shoulder peak at low frequency is an indication of the longer relaxation time pertinent to macromolecules. It is clear that as the frequency and temperature increase,  $\tan \delta$  maximum does not shift toward higher frequencies but its magnitude increases. These well-known features are characteristics of the freezing of dipolar motion with no longer-range correlations (i.e., glass-like).

The temperature dependence of  $\tan \delta$  at some selected frequencies (1, 10, and 100 kHz) for all network samples is shown in Figure 7(a–c). From the figure, it is observed that  $\tan \delta$  increases with the increase of frequency. Cu-PyzPz exhibits a higher  $\tan \delta$ . The behavior of  $\tan \delta$  reflects the presence of relaxing dipoles in all samples. Since the strength and frequency of relaxation depend on these relaxing dipoles, the loss tangent peak shifts toward higher temperature with increasing frequencies. The relaxation peak is observed for all investigated networks at 348, 363, and 378 K and  $f$  is equal to 1, 10, and 100 kHz, respectively. It is found that the shape of the full width at half of the peak height changes slightly in the studied range of frequencies and selected temperatures.

#### Ac conductivity

The major aspects of conductivity mechanisms in polymeric systems are charge carrier generation and transport, the latter is especially difficult in

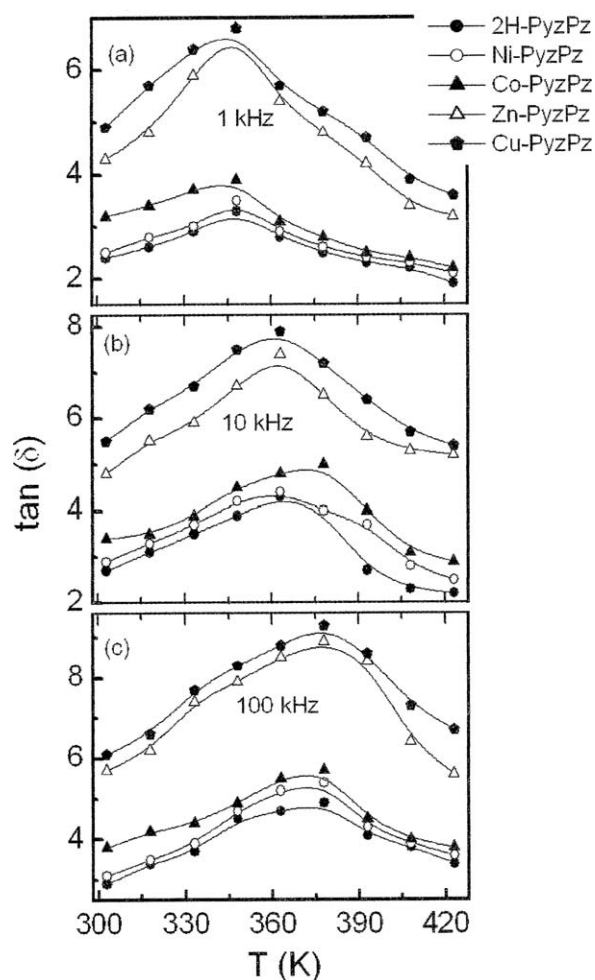


**Figure 7** The temperature dependence of  $\tan \delta$  for 2H-PyzPz and M-PyzPz samples at different frequencies: (a) 1.0 kHz, (b) 10 kHz, and (c) 100 kHz.

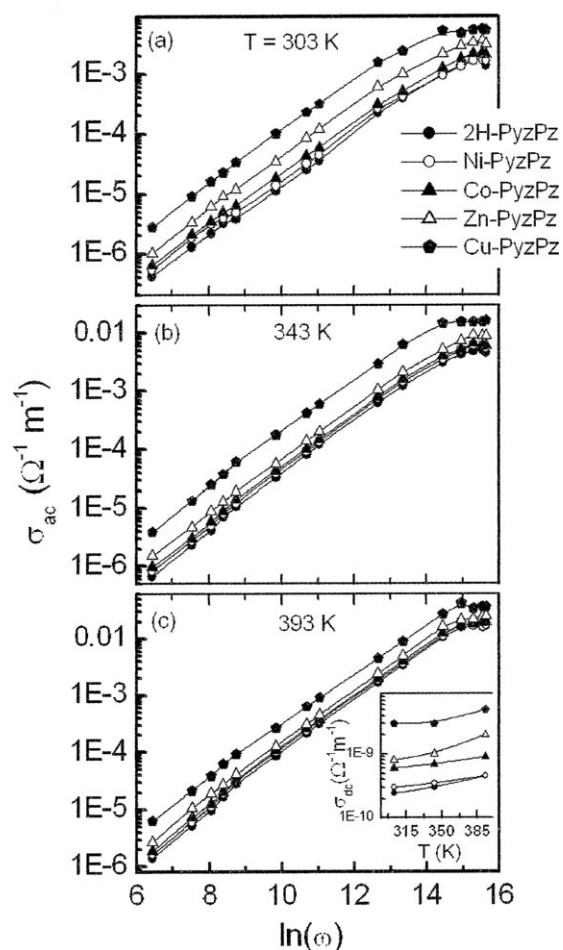


**Figure 8** The frequency dependent of ac conductivity,  $\sigma_{ac}$ , for 2H-PyzPz and M-PyzPz samples at different temperatures: (a)  $T = 303$  K, (b)  $T = 343$  K, and (c)  $T = 393$  K. The inset in (c) shows the temperature dependence of the estimated dc conductivity,  $\sigma_{dc}$ , for all studied samples.

investigation and interpretation. There are several models describing the origin and nature of the charge carriers in polymer networks, which take into account the specific electronic structure of a given polymer. The lack of long order in most polymer systems does not allow extension of such treatments to describe their actual macroscopic electronic properties completely. Rather, the observed bulk

conductivity of polymeric materials is a complex function of the number of charge carriers and their transport along polymer chains and morphological barriers. It can also mention here that the electrons in conjugated systems are loosely bound to be able to jump around the polymeric chains so that the conductivity increases.

The double logarithmic plot of the frequency dependence of ac conductivity,  $\sigma_{ac}(\omega)$ , at three selected temperatures ( $T = 303, 343,$  and  $393$  K) is presented in Figure 8(a–c). As seen,  $\sigma_{ac}(\omega)$  increases monotonically with increasing frequency ( $0.1 \text{ kHz} \leq f \leq 500 \text{ kHz}$ ) and eventually attains a high frequency plateau. Within this range of frequency, no relaxation peak was identified. In addition, all samples exhibit high conductivity and the difference between 2H-PyzPz and M-PyzPz (except for  $M = \text{Cu}$ ) is still small at  $T \geq 343$  K. A common feature of the dielectric materials is the frequency-dependent conductivity given by the well-known universal dynamic response<sup>36,37]</sup>

$$\sigma_t = \sigma_{dc} + \sigma_{ac}(\omega) \quad (2)$$

$$\sigma_{ac}(\omega) = \sigma_t - \sigma_{dc} = B\omega^s \quad (3)$$

where  $\sigma_{dc}$  is the dc (or low frequency), conductivity,  $\sigma_t$  is the total conductivity,  $s$  is the universal exponent and  $B$  is a pre-exponential factor. The dc conductivity is calculated using the low-frequency region and extrapolating  $\sigma(\omega)$  to the  $f \rightarrow 0$ . The inset in Figure 8(c) displays the change of  $\sigma_{dc}$  with temperature for all network samples. One notes that Cu-PyzPz exhibits the highest  $\sigma_{dc}$  compared to other investigated samples. The frequency-dependent conductivity is found to be the best represented by eq. (3). The values of  $s$  and  $B$  are listed in Table II and are slightly temperature dependent. It is clear from this table that  $s < 1$  at  $T = 303$  K and  $s \geq 1.0$  with increasing temperatures. The values of  $s$ , which less than unity are found to be consistent with that observed in many hopping systems.<sup>21,38</sup> The conduction mechanism of the samples that have  $s > 1.0$  (less than 2) may be corresponding to the well-localized hopping and/or reorientational motion.<sup>39</sup>

**TABLE II**  
The Fit Results, ( $s$  and  $B$ ), According to eq. (3) for All Network Samples at Some Selected Temperatures

Samples	$T = 303$ K		$T = 343$ K		$T = 393$ K	
	$B$	$s$	$B$	$s$	$B$	$s$
2H-PyzPz	9.818E – 10	0.953 ± 0.01	1.028E – 9	1.039 ± 0.02	1.629E – 9	1.089 ± 0.02
Ni-PyzPz	1.865E – 9	0.909 ± 0.02	1.257E – 9	1.034 ± 0.02	1.916E – 9	1.084 ± 0.02
Co-PyzPz	2.019E – 9	0.922 ± 0.01	1.484E – 9	1.028 ± 0.02	2.317E – 9	1.073 ± 0.02
Zn-PyzPz	3.559E – 9	0.923 ± 0.02	2.645E – 9	1.007 ± 0.01	3.830E – 9	1.051 ± 0.01
Cu-PyzPz	7.271E – 9	0.953 ± 0.02	5.784E – 9	1.037 ± 0.01	1.026E – 8	1.024 ± 0.01

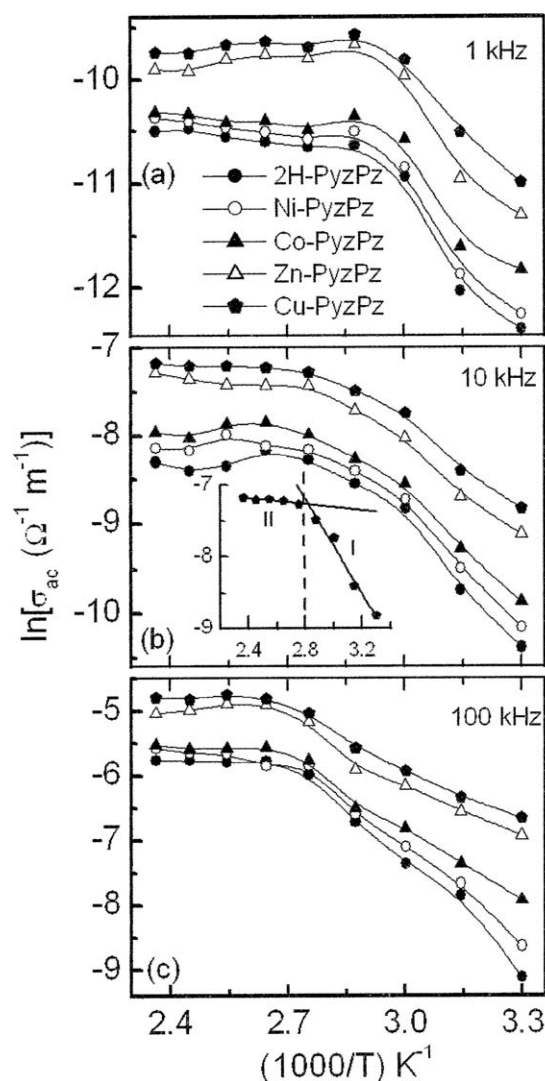


**Figure 9** The temperature dependence of ac conductivity,  $\sigma_{ac}$ , at different frequencies: (a) 1.0 kHz, (b) 10 kHz, and (c) 100 kHz. The inset in (b) represents  $\ln(\sigma_{ac})$  versus  $1000/T$ , and the solid lines show the fit in region I and II.

The temperature dependence of the conductivity presented as  $\ln(\sigma_{ac})$  versus the reciprocal temperature at some selected frequencies (1, 10, and

100 kHz) is shown in Fig. 9(a–c).  $\ln(\sigma_{ac})$  exhibits two straight regions (I and II) and shows an increase with increasing temperatures in region I ( $303 \text{ K} \leq T \leq 348 \text{ K}$ ). Generally, the ac conductivity is thermally activated according to the Arrhenius relation:

$$\sigma_{ac} = A \exp(-E/kT) \quad (4)$$

where  $A$  is the pre-exponential factor,  $E$  is the activation energy  $k$ , and  $T$  have their usual meaning. The increase of  $\sigma_{ac}$  with temperature may be due to the increase of the absorbed energy, which leads to increase the number of the charge carriers that contribute to the conduction process. This reveals that the conduction mechanism could be a hopping one.<sup>40</sup> Also, the variation of the conductance with temperature can be attributed to a combined effect of a change in the conductance with temperature and to the nature of the trap distribution inside the polymer networks. It was found that the temperature dependence of  $\sigma_{ac}$  in I and II regions obeys eq. (4), so the values of  $E$  are calculated and listed in Table III. The inset in Figure 9(b) displays the fit of  $\ln(\sigma_{ac})$  of Cu-PyzPz for instance. As seen from Table III, the  $E$  values in region I, are higher than those in region II. The  $\sigma$ - $T$  curves of all investigated samples in region II are associated with very small  $E_{II}$  (0.01–0.04 eV) consistent with hopping of charge carriers between localized states.<sup>41,42</sup> The low values of activation energy suggested a transitional region between hopping and another conduction process presumably free band conduction. On the other hand, the values of  $E_I$  in region I are 0.2 – 0.5 eV. These values are also consistent with that reported on zinc phthalocyanine thin films.<sup>43</sup> Anyway, such results are in reasonable agreement with those obtained for other phthalocyanine compounds.<sup>44–46</sup> Once again, the special conjugation in pyrazinoporphyrazines may be one of the reasons that these polymers exhibit a conductive behavior.

**TABLE III**  
The Activation Energies for 2H-PyzPz and M-PyzPz Samples According to the Fit of Arrhenius Equation in Two Regions; I ( $303 \text{ K} \leq T \leq 348 \text{ K}$ ) and II ( $348 \text{ K} \leq T \leq 422 \text{ K}$ )

Samples	$f = 1 \text{ kHz}$		$f = 10 \text{ kHz}$		$f = 100 \text{ kHz}$	
	$E_I$ (eV)	$E_{II}$ (eV)	$E_I$ (eV)	$E_{II}$ (eV)	$E_I$ (eV)	$E_{II}$ (eV)
2H-PyzPz	0.38	0.031	0.389	0.025	0.466	0.040
Ni-PyzPz	0.379	0.029	0.367	0.024	0.404	0.065
Co-PyzPz	0.329	0.037	0.336	0.010	0.291	0.041
Zn-PyzPz	0.359	0.032	0.296	0.031	0.209	0.019
Cu-PyzPz	0.303	0.017	0.283	0.018	0.222	0.043

## CONCLUSIONS

Both conductive new full-conjugated 2H-PyzPz and M-PyzPz network polymers have been successfully synthesized. Both molecular masses and metal contents of these synthesized polymer networks confirm the efficiency of tetramerization polymerization and complexation reactions. The dielectric constants,  $\epsilon'$ , of all investigated samples (2H-PyzPz and M-PyzPz) were found to decrease with the increase in frequency and increase with the increase in temperature. The loss tangent,  $\tan \delta$ , shows relaxation processes and exhibits frequency as well as temperature dependence. The ac conductivity,  $\sigma_{ac}$ , was found to vary as  $\omega^s$  and the exponent,  $s$ , were less than unity around room temperature indicating a dominant correlated barrier hopping mechanism. With increasing temperatures,  $s$  was found to be equal or higher than unity and the conduction may correspond to the well-localized hopping and/or reorientational motion. At  $303 \text{ K} \leq T \leq 348 \text{ K}$ , the conductivity is thermally activated with activation energy,  $E$ , of 0.2–0.5 eV, whereas  $E$  is very small (0.01–0.04 eV) at  $348 \text{ K} \leq T \leq 423 \text{ K}$ . The addition of metals may affect the charge carriers causing higher conductivity. Finally, research effort is seriously required to understand fully the optical behaviors of these compounds due to their importance in technology and industry.

## References

- Jörg, K.; Subramanian, L. R.; Michael, H. J. *Porphyrins Phthalocyanines* 2000, 4, 498.
- Sakamoto, K.; Ohno-Okumura, E.; Kato, T.; Watanabe, M.; Cook, M. J. *Metal-based drugs* 2008, 2008, 1.
- Sharman, W. M.; J. E. van Lier, J. *Porphyrins Phthalocyanines* 2000, 4, 441.
- Leznoff, C. C. In: *Phthalocyanines 2 Properties and Applications*; Leznoff, C. C.; Lever, A. B. P., Eds.; VCH, 1989; Vol. 1, p 1.
- Faust, R.; Weber, C. *J Org Chem* 1999, 64, 2571.
- Wang, C. S.; Bryce, M. R.; Batsanov, A. S.; Howard, J. A. K. *Chem A Eur J* 1997, 3, 1679.
- Donzello, M. P.; Ou, Z.; Monacelli, F.; Ricciardi, G.; Rizzoli, C.; Ercolani, C.; Kadish, K. M. *Inorg Chem* 2004, 34, 8626.
- Mitzel, F.; Gerald, S. F.; Beeby, A.; Faust, R. *Chem Eur J* 2003, 5, 1233.
- Rusanova, J.; Pilkington, M.; Decurtins, S. *Chem Commun* 2002, 2236.
- Kim, J.; Jaung, J. Y.; Ahn, H. *Macromol Res* 2008, 16, 367.
- Budd, P. M.; McKeown, N. B.; Fritsch, D. *J Mater Chem* 2005, 15, 1977.
- Budd, P. M.; Ghanem, B.; Msayib, K.; McKeown, N. B.; Tattershall, C. *J Mater Chem* 2003, 13, 2721.
- Kingsborough, R. P.; Swager, T. M. *Angew Chem* 2000, 112, 3019.
- Mott, N. F.; Davis, E. A. *Electronic Processes in Non-Crystalline Materials*; Clarendon Press, Oxford, 1971.
- Farid, A. M.; Bekheet, A. E. *Vacuum* 2000, 59, 932.
- Bodjema, B.; Guillard, G.; Gamoudi, M.; Maitrot, M.; Andre, J. J.; Martin, M.; Simon, J. *J Appl Phys* 1984, 56, 2323.
- El-Nahass, M. M.; El-Deed, A. F.; Abd-El-Salam, F. *Org Elect* 2006, 7, 261.
- Riad, A. S.; Korayem, M. T.; Abdel-Malik, T. G. *Physica B* 1999, 270, 140.
- Shihub, S. I.; Gould, R. D. *Thin Solid Films* 1995, 254, 187.
- Nalwa, H. S.; Vazudevan, P. *J Mater Sci Lett* 1983, 2, 22.
- Saleh, A. M.; Gould, R. D.; Hassan, A. K. *Phys Stat Sol A* 1993, 139, 379.
- Saad, E. A. I. *J Optoelectr Adv Mater* 2005, 7, 3127.
- Gould, R. D.; Hassan, A. K. *Thin Solid Films* 1993, 223, 334.
- Abdel-Malik, T. G.; Adel-Latif, R. M.; El-Shabasy, M.; Abdel-Hamid, M. *Ind J Phys* 1988, 62A, 17.
- Yamato, T.; Fujimoto, M.; Miyazawa, A.; Matsuo, K. *J Chem Soc Perkin Trans* 1997, 1, 1201.
- Hu, J.; Zhang, D.; Harris, F. W. *J Org Chem* 2005, 70, 707.
- J-Jaung, Y.; Matsuoka, M.; Fukunishi, K. *Synthesis* 1998, 1998, 1347.
- Puigdollers, J.; Voz, C.; Fonrodona, M.; Cheylan, S.; Stella, M.; Andreu, J.; Vetter, M.; Alcubilla, R. *J Non-Cryst Solids* 2006, 352, 1778.
- Wizel, S.; Margel, S.; Gedanken, A.; Rojas, T. C.; Fernandez, A.; Prozorov, R. *J Mater Res* 1999, 14, 3913.
- Bruder, I.; Schöneboom, J.; Dinnebier, R.; Ojala, A.; Schäfer, S.; Sens, R.; Erk, P.; Weis, J. *Org Electron* 2010, 11, 377–387.
- Cory, M. G.; Zerner, M. C. *Chem Rev* 2001, 91, 813–822.
- Chen, Q.; Gu, D.; Gan, F. *Physica B* 1995, 212, 189.
- Pradhan, D. K.; Choudhary, R. N. P.; Samantaray, B. K. *Int J Electrochem Sci* 2008, 3, 597.
- El-Nahass, M. M.; Farid, A. F.; Abd El-Rahman, K. F.; Ali, H. A. M. *Physica B* 2008, 403, 2331.
- Talwar, I. M.; Sinha, H. C.; Shrivastava, A. P. *J Mat Sci Lett* 1985, 4, 448.
- Elliott, S. R. *Phys Amorphous Mater*; Wiley, New York, 1983.
- Jonscher, A. K. *Dielectric Relaxation in Solids*; Chelsea Dielectric Press: London, 1983; p 340.
- Bahri, R.; Singh, H. P. *Thin Solid Films* 1979, 62, 2911; 1980, 69, 281.
- Funggao, C.; Saunders, G.; Wei, Z.; Allmond, D.; Coutrone M.; Mandanici, C. *Solid State Ionics* 1998, 109, 89.
- Hanafy, T. A. *Curr Appl Phys* 2008, 8, 527.
- Jonscher, A. K. *Thin Solid Films* 1976, 36, 1.
- Le Moigne, J.; Evevn, R. *J Chem Phys* 1985, 83, 6472.
- Abu-Hilal, A. O.; Saleh, A. M.; Gloud, R. D. *Mater Chem Phys* 2005, 94, 165.
- Nalwa, H. S.; Vazudevan, P. *J Mater Sci Lett* 1983, 2, 22.
- Amar, N. M.; Saleh, A. M.; Gould, R. D. *Appl A* 2003, 76, 77.
- Hassan, A. K.; Gould, R. D. *Int J Electron* 1993, 74, 59.